



Published in final edited form as:

Cancer Res. 2010 March 1; 70(5): 1885–1895. doi:10.1158/0008-5472.CAN-09-2833.

Talin1 Promotes Tumor Invasion and Metastasis via Focal Adhesion Signaling and Anoikis Resistance

Shinichi Sakamoto¹, Richard O. McCann², Rajiv Dhir³, and Natasha Kyprianou^{1,4,5}

¹Department of Surgery/Urology, University of Kentucky College of Medicine

²Department of Mercer University School of Medicine, Division of Basic Medical Sciences, Macon, GA

³Department of Pathology, University of Pittsburgh Medical Center, Pittsburgh, PA

⁴Department of Molecular & Cellular Biochemistry, University of Kentucky College of Medicine, Lexington, KY.

⁵Markey Cancer Center, University of Kentucky College of Medicine, Lexington, KY.

Abstract

Talin1 is a focal adhesion complex protein that regulates integrin interactions with the extracellular matrix (ECM). This study investigated the significance of talin1 in prostate cancer progression to metastasis *in vitro* and *in vivo*. Talin1 overexpression enhanced prostate cancer cell adhesion, migration and invasion by activating survival signals and conferring resistance to anoikis. ShRNA-mediated talin1 loss led to a significant suppression of prostate cancer cell migration and transendothelial invasion *in vitro* and a significant inhibition of prostate cancer metastasis *in vivo*. Talin1 regulated cell survival signals via phosphorylation of focal adhesion complex proteins such as focal adhesion kinase (FAK) and Src, and downstream activation of AKT. Targeting AKT activation led to a significant reduction of talin1-mediated prostate cancer cell invasion. Furthermore, talin1 immunoreactivity directly correlated with prostate tumor progression to metastasis in the TRAMP mouse model. Talin1 profiling in human prostate specimens revealed a significantly higher expression of cytoplasmic talin1 in metastatic tissue compared to primary prostate tumors ($P < 0.0001$). These findings suggest: (a) a therapeutic significance of disrupting talin1 signaling/focal adhesion interactions in targeting metastatic prostate cancer and (b) a potential value for talin1 as a marker of tumor progression to metastasis.

Keywords

Prostate cancer; Talin1; Invasion; Metastasis; Anoikis; Focal Adhesions

INTRODUCTION

Cancer metastasis is a multistep and complex process that involves dissociation of the tumor cells from the organ of origin, degradation of the extracellular matrix (ECM), cell migration, anchorage-independent growth, apoptosis evasion, angiogenesis, invasion of surrounding tissues, cell adhesion, movement and colonization to distant sites in the body (1). Human prostate cancer progression to advanced metastatic disease is associated with relapse to a

hormone-refractory state due to impaired apoptotic response to androgen ablation. Androgen-independent prostate cancer cells become resistant due to roadblocks in apoptosis and depending on the interactions with the tumor microenvironment, acquire invasive and metastatic properties (2). Both tumor epithelial and endothelial cells require attachment to the ECM for survival and upon loss of adhesion, they undergo detachment-induced cell death, known as anoikis. Anoikis, a unique phenomenon of apoptosis consequential to insufficient cell-matrix interactions(3) is recognized as a significant player in tumor angiogenesis and metastasis(4). During metastatic progression, cells are in a dynamic state lacking firm attachment to the ECM and susceptible to anoikis (4). Thus, resistance to die via anoikis dictates tumor cell survival and provides a molecular basis for therapeutic targeting of metastatic prostate cancer.

Talin1 is a focal adhesion protein that binds to multiple adhesion molecules including integrins, vinculin, focal adhesion kinase(FAK) and actin. In addition to structural role, talin1 play essential role in integrin activation(5). Upon activation, integrins increase the functional interactions between a cell and the ECM, thus serves as bidirectional transducers of extracellular and intracellular signals, ultimately regulating adhesion, proliferation, anoikis, survival and tumor progression(5-8). Therefore, talin1 mediated linkage of integrins to the actin cytoskeleton in focal adhesion complexes is a dynamic, multicomponent plasma membrane-associated assemblies essential for cell adhesion and motility (9). Talin1-deficient mice exhibit failure of integrins to aggregate into clusters and connect to the cytoskeleton, resembling the integrin deficient phenotype, and supporting that integrin function is talin1-dependent (10). Recent evidence documents that talin1 suppresses expression of E-cadherin, a cell-cell adhesion effector that negatively correlates with cancer progression, independent of integrin (11), indicating a role for talin1 distinct from the integrin-dependent mechanism. However, the precise role of talin1 in cancer development and progression has not been elucidated.

The present study investigated the role of talin1 in prostate cancer progression to metastasis. We demonstrate that talin1 engages in focal adhesion interactions with the AKT signaling as the intracellular survival mechanism to confer anoikis resistance and promote prostate cancer cell invasion. Talin1 profiling in human prostate cancer specimens revealed a significantly increased talin1 expression in metastases compared to benign and primary prostate tumors.

MATERIALS AND METHODS

Cell Culture and Transfections

Human prostate cancer cell lines PC-3, DU-145, LNCAP, CWR-22, were obtained from the American Type Tissue Culture Collection (Rockville, MD) and cultured in RPMI-1640 (Invitrogen, Carlsbad, CA) containing 10% fetal bovine serum (Invitrogen) and antibiotics, PenicillinG/Streptomycin (50µg/ml). Human vascular endothelial cells (HUVEC) and Human Microvascular Brain Endothelial cells (HBMEC) were cultured in endothelial basal medium (EGM-2) (Cambrex, East Rutherford, New Jersey). Transfection was performed using Lipofectamin™ 2000 reagent (Invitrogen, Carlsbad, CA) according to the manufacturer's protocol. PC-3 cells were transfected with pEGFP or GFP-Talin1 plasmids and cloned under G418 selection (Geneticin, Gibco Brl, Grand Island, NY). For silencing talin1 expression in prostate cancer cells, the ShRNA talin1 vector (GIPZ ShRNAmir talin1) was obtained from Open Biosystems (Huntsville, AL). After transfection ShRNA talin1 DU-145 cells were selected using puromycin (a resistance marker). Polyclonal populations were pooled under antibiotic selection media and after several passages, stable cell lines were characterized for each group by Western blotting.

Attachment Assay

Cells were seeded in six-well plates (5×10^4 cells/well) coated with fibronectin (BD Biosciences Discovery Labware, Bedford, MA). Following a 10-min attachment period, attached cells were fixed with methanol (100%) and stored at 4°C in PBS for image analysis. Cells were counted in three $\times 100$ fields/well.

Migration Assay

Cell cultures (at 75% confluency) were subjected to wounding as previously described (12). At 24 and 48hrs post-wounding cells migrating to the wounded areas were counted under the microscope.

Transendothelial Migration (TEM) Assay

Sterile (12mm diameter) glass coverslips were coated with Matrigel (Becton Dickson, Franklin Lakes, NJ). Coverslips were then seeded (at a density of 6.25×10^4 HBMEC) to form a complete monolayer. Cells were allowed to adhere/spread on the Matrigel for 24hrs prior to initiation of the migration assay. PC-3 and DU-145 cells were resuspended in EGM-2MV (Cambrex) and added to the HBMEC monolayer (8×10^3 cells/coverslip), for 12hrs. Cells were subsequently fixed in paraformaldehyde (2% in PBS) (10mins at room temperature) and washed with PBS. Nuclei were stained with DAPI Nucleic Acid Stain (Molecular Probes, Eugene, OR). Slides were visualized and examined under confocal microscopy.

Western Blot Analysis

Protein expression was determined by immunoblotting using the following specific antibodies: The human polyclonal rabbit talin1 antibody was generated by Dr. Richard McCann. The antibodies against FAK, AKT, phospho-Akt(Ser473), p44/42-MAP kinase, phospho p42/44-MAP kinase, GSK3 β , phosphoGSK3 β , SRC and Phospho-SRC(Tyro416) were obtained from Cell Signaling Technology (Beverly, MA); phospho-FAK(Y397) was obtained from Sigma (St. Louis, MO). Protein levels were normalized to α -actin expression, detected by using the α -actin antibody from Oncogene Research Products™ (La Jolla, CA). Cell lysates were prepared RIPA buffer [150 mmol/l NaCl, 50 mmol/l Tris (pH 8.0), 0.5% deoxycholic acid, 1% NP-40 with 1 mmol/l phenyl methyl-sulfonyl fluoride]. Protein content was quantified using the bicinchoninic acid (BCA) protein assay kit (Pierce, Rockford, IL) and protein samples (30 μ g) were subjected to SDS-PAGE and transferred to Hybond-C membranes (Amersham Pharmacia Biotech, Piscataway, NJ). Membranes were blocked in 5% milk in TBS-T (TBS containing 0.05% Tween 20) (1 hr at room temperature) and following incubation with the respective primary antibody (overnight at 4°C), membranes were exposed to species-specific horseradish peroxidase-labeled secondary antibodies. Signal detection was achieved with SuperSignal West Dura Extended Duration Substrate (Pierce) and visualized using a UVP Imaging System. Fold change in specific protein expression was determined on the basis of α -actin expression as a loading control.

Immunoprecipitation

DU-145 cells, ShVector control and ShTalin1 transfectants were lysed in RIPA buffer. Total protein concentration was quantified (as described above) and protein samples (100 μ g) were incubated overnight at 4°C with the specific antibody. Controls for the immunoprecipitations were set up by using control IgG derived from the same species as the primary antibody + Protein G/A (2nd antibody). Following incubation of lysates with Protein G Plus/Protein A agarose beads (30 μ l) for 3hrs at 4°C, beads were washed in PBS buffer, subjected to SDS-PAGE analysis, and transferred to nitrocellulose membranes (Amersham Pharmacia).

AKT inhibitor

The AKT inhibitor; 1L6-Hydroxymethyl-chiro-inositol-2-(R)-2-O-methyl-3-O-octadecyl-sn-glycerocarbonate, was obtained from Calbiochem (Gibbstown, NJ); it was used at concentration of $10\mu\text{ M}$ as previously reported (13).

Apoptosis Evaluation

Cells were harvested in EDTA buffer (0.5mM) and incubated in Hanks Balanced Salt Solution (HBSS) supplemented with 2% BSA and 0.01% sodium azide (30mins at 4°C). Cells were subsequently fixed in 4% (w/v) formaldehyde in PBS, and exposed to Annexin-V (R&D Systems, Minneapolis, MN) followed by FITC-conjugated secondary antibody. Analysis of Annexin V fluorescence was performed using flow cytometry (Partec, Munster, Germany).

Caspase-3 Activity Assay

GFP talin1 and vector control cells were plated on either collagen or nonadhesive polyhydroxyethylmethacrylate (poly-HEMA) and incubated for 6-24hr. Caspase-3 activation were measured by Caspase-Glo 3/7 Assay (Promega Madison, WI) according to manufacturer's protocol. Exposure to TRAIL (100ng) + Velcade (100nM) for 16hrs was used as a positive control.

Cell Cycle Arrest Evaluation

Cells were fixed with 70% ethanol (30mins at 4°C), stained with Propidium iodide (50 $\mu\text{g/ml}$) containing 20 $\mu\text{g/ml}$ of RNase (30mins at room temperature) and were subsequently subjected to flow-cytometric analysis. Cell cycle progression was analyzed via fluorescence-activated cell sorting (FACS) using the Partec Flow Max.

Anoikis Evaluation

Cells were plated on fibronectin or the nonadhesive polyhydroxyethylmethacrylate (poly-HEMA)-coated dishes and incubated for 24hrs. Cells undergoing apoptosis were detected using the Annexin V immunofluorescence approach and flow-cytometric analysis (Partec). Western blotting was used to determine expression of apoptosis regulators after talin1 overexpression/silencing in prostate cancer cells.

Caspase-3 Activity Assay

GFP talin1 and vector control cells were plated on either collagen or nonadhesive polyhydroxyethylmethacrylate (poly-HEMA) and incubated for 6-24hr. Caspase-3 activation were measured by Caspase-Glo 3/7 Assay (Promega Madison, WI) according to manufacturer's protocol. Exposure to TRAIL (100ng) + Velcade (100nM) for 16hrs was used as a positive control.

In Vivo Experimental Metastasis Assay

Human prostate cancer cells were injected (2×10^6 cells /80 μl of PBS) in the tail vein of male nude mice (4–6 wks). After 4-weeks mice were sacrificed and the lungs and liver were surgically excised and examined for metastatic lesions under a dissecting microscope (40 \times).

TRAMP Transgenic Mouse Model

The TRAMP mice (C57BL/6J) are transgenic mice that express SV40T/t antigens under the prostate specific rat probasin promoter(14), (15). TRAMP transgenic males develop prostate adenocarcinoma in a manner resembling the clinical progression of human prostate cancer from intra-epithelial neoplasia to androgen-independent metastatic tumors. Hematoxylin and

eosin (H&E)-stained sections of prostate tissues from TRAMP/+/+ male mice were evaluated by two independent investigators (S.S. and N.K.) to confirm pathological grade. Wild-type male mice (C57BL/6) of comparable age groups (6-29wks) served as controls. The histopathological grading of prostatic tumors was conducted using a standard grading scale in TRAMP mice. Flat lesions and focal cell piling (grade 2.0-2.2) were observed in the majority of 12wks-old TRAMP mice (Table 1). In 20wk-27wk-old TRAMP mice, prostates exhibited focal cribriform lesions protruding into the lumen (grade 3-5), representing tumor progression to advanced disease.

Prostate sections from wild type and the TRAMP tumors of increasing grade and metastatic lesions (5 μ m), were subjected to immunohistochemical analysis for talin1 expression using the talin1 polyclonal antibody (provided by Dr. McCann). Slides were examined under a Nikon fluorescence microscope (Nikon Inc., Melville, NY). Values were determined in a semiquantitative fashion, incorporating both the intensity of staining and the number of positively stained epithelial cells (16). Briefly, the staining intensity (I) was graded as 0, absent; 1, weak; 2, moderate; or 3, strong. The proportion (P) of positive epithelial cells (0.0 to 1.0) with the staining intensity was recorded; A score for each histological grade (H) was determined as the product of intensity and proportion ($H = I \times P$).

Human Prostate Specimens

Human prostate tissue specimens from patients with primary and metastatic prostate tumors (Department of Pathology, University of Pittsburgh), were subjected to immuno-profiling for talin1 expression. Computer-image analysis determined talin1 expression levels in prostate specimens: 74 normal prostate; 93 normal areas surrounding malignant tissue; 71 BPH areas; 35 prostate primary tumors (Gleason Score range 6-9); and 44 metastatic lesions.

Statistical Analysis

One-way analysis of variance (ANOVA) was performed using the StatView statistical program to determine the statistical significance between values (P value less than 0.05). Tissue immunoreactivity was analyzed and interpreted according to previously published protocols (17).

RESULTS

Role of Talin 1 in Prostate Tumorigenesis

The expression profile of talin1 was assessed during *in vivo* prostate tumorigenesis in the transgenic adenocarcinoma mouse prostate (TRAMP) model. As shown in Figure 1A, talin1 immunoreactivity was primarily detected among the glandular epithelial cells in the TRAMP prostates. Talin1 protein levels progressively increased with increasing age of TRAMP mice (6-27wks) [Fig. 1, panel A (iii-vi)]. There was weak talin1 immunoreactivity in prostate tissue from wild-type (WT) control mice, while the intensity of talin1 staining was considerably stronger in primary prostate tumors, with the highest detected in liver metastases [Fig.1A (ii)]. Quantitative analysis revealed a 2-fold increase in talin1 levels in prostate tumors derived from 12wk-TRAMP mice, compared to the 6wk old TRAMP (Fig. 1B). By 27-wks of age, at which time TRAMP mice exhibit a highly aggressive prostate tumor phenotype (grade 4.5-5), talin1 expression increased significantly ($P=0.0019$) (Fig. 1B).

Talin1 Correlates with Human Prostate Cancer Progression

To determine significance of talin1 in human prostate cancer progression to metastatic disease, we conducted immunohistochemical staining for talin1 in human prostate tissue specimens (Fig. 1, panel C). Talin1 expression was analyzed in 307 human prostate tissue specimens

including 74 normal, 101 adjacent areas to the tumor, 56 benign prostate hyperplasia (BPH), 34 primary tumors (Gleason 6-9) and 74 metastatic lesions (Table 1a). Immunoreactivity was quantitated by automated quantitative analysis to determine the cytoplasmic levels of talin1. A representative picture of normal prostate, BPH, primary prostate tumor and metastatic lesion to the lymph node is shown on Figure 1C (Panels i-iv). Cytoplasmic talin1 expression was significantly higher in primary tumor and metastasis lesion compare to normal prostate ($P < 0.00028$, $P < 0.0001$, respectively), while talin1 expression detected in BPH specimens was comparable to those detected in normal prostate tissue ($P = 0.319$). Talin1 expression in metastatic lesions was significantly higher compared to primary tumors ($P < 0.0001$) (Table 1a). The intensity of talin1 immunoreactivity in poorly differentiated prostate tumors (Gleason 8/9) was significantly higher compared to moderately differentiated tumors (Gleason 6/7) ($P = 0.0009$). Talin1 levels also increased with increasing Gleason Score (Gleason 6/7 to 9) (Table 1b).

Talin 1 Promotes Prostate Cancer Cell Adhesion, Migration and Invasion

The effect of talin1 overexpression on the adhesion ability and migration potential of prostate cancer cells were examined *in vitro*. The endogenous expression of talin1 was profiled in human prostate cell lines as well as prostate fibroblasts (as positive control for talin1 abundance). DU-145 prostate cancer cells exhibited the highest talin1 expression (Fig. 2A). GFP-talin1 stable transfectants were generated in PC-3 cells which express very low endogenous talin1 levels (Fig. 2, panel A). Overexpression of talin1 (Fig. 2A, right panel), significantly increased both the adhesion (Fig. 2B) and migration potential of prostate cancer cells (Fig. 2C) compared to vector control cells. To determine the consequences of talin1-overexpression on the invasive potential of prostate cancer cells through an endothelial cell monolayer, the trans-endothelial migration (TEM) assay was performed using the human brain membrane endothelial cells (HBMEC). As shown on Figure 2D, talin1 overexpression led to a significant increase in prostate cancer cell invasion through the endothelial cell monolayer ($p < 0.01$).

Prostate tumor epithelial cell survival requires continuous attachment to the ECM and it is recognized that fibronectin, laminin and collagen participate in the formation of attachment plaques linked to the actin cytoskeleton. The impact of talin1 loss on prostate cancer cell adhesion was examined by generating ShRNA-talin1 stable transfectants in DU-145 prostate cancer cells that are characterized by high endogenous talin1 expression (Fig.3, panel A). As shown on Fig 3A, ShRNA silencing of talin1 effectively reduced talin1 expression in DU-145 cells (>80%). Talin1 silenced DU-145 cells exhibited a reduced ability to adhere to different ECM components including collagen, laminin and fibronectin (Fig. 3B). Furthermore loss of talin1 led to significant reduction in the migration potential compared to vector control cells (Fig. 3C). Examination of the invasion ability of talin1-silenced transfectants through an endothelial cell monolayer revealed a significant suppression (Fig. 3D).

Talin1 Facilitates ECM-integrin Mediated Focal Adhesion Signals

The mechanism via which talin1 activates intracellular signals was investigated in the context ECM-epithelial cell interaction. We focused on FAK/AKT signaling and the intracellular MAP kinase pathway as both have been implicated in integrin-focal adhesion dependent signals (18). Activation of FAK due to phosphorylation (Y397) was observed on collagen attachment conditions, while it was more prominent on fibronectin coated ECM in talin1 overexpressing cells relative to control cells (Fig. 4A). Talin1 overexpression in prostate cancer cells PC-3, also resulted in a marked activation on phosphorylation of AKT (Ser473) under fibronectin-attachment conditions, while only a modest activation of p44/42 MAP kinase was observed (Fig. 4A). These observations were confirmed by fluorescence microscopy (data not shown). There was a significant enhancement in the phosphorylation of FAK, AKT and MAPK when

cells were cultured on fibronectin-coated surface (Fig. 4B). Talin1 overexpression induced AKT phosphorylation as early as 3hrs after adhesion, with continuous activation after 24hrs (Fig. 4B, right panel).

The effect of talin1 on integrin-focal adhesion complex signaling interactions was subsequently investigated, by examining the direct binding of talin1 to integrin $\beta 3$, a key talin1 binding partner (19). To this end we used the DU-145 cell line, which exhibits high endogenous expression of integrin $\beta 3$ (data not shown). Talin1 silencing significantly reduced talin1 binding to integrin $\beta 3$, as well as the focal adhesion partners, FAK and Src (Fig. 4C). The reduced binding of Src upon talin1 loss (Fig. 4C), led us to probing the role of ILK-1, a protein that regulates Src binding in response to integrin activation. Immunoprecipitation by integrin $\beta 3$ revealed a significant decrease in ILK-1 binding in talin1-silenced prostate cancer cells. Immunoprecipitation by ILK-1 revealed that talin1 loss abrogated ILK-1 binding to integrin $\beta 3$ complex (Fig. 4C, right panel). In the presence of a blocking antibody against integrin $\beta 3$ there was a significant reduction in phosphorylation of AKT and FAK in talin1 overexpressing cells (Fig. 4D).

Talin1 Mediates Anoikis Resistance

In order to investigate the integrin-independent role for talin1 (11), we examined the impact of talin1 overexpression on cell-suspension conditions. Cells were plated on either fibronectin-coated matrix or the nonadhesive polyhydroxyethylmethacrylate (poly-HEMA). As shown on Figure 5 (Panel A), talin1 did not lead to a significant apoptotic effect in adherent conditions, but under non-adherent conditions, talin1 overexpressing cells exhibited a significant reduction in apoptosis as detected by Annexin V staining (Fig. 5A), suppression of caspase-3 activity (Fig. 5B), activation of AKT survival signaling (Fig. 5C), as well as subpopulation G0-G1 arrest (Supplemental Figure 1). Talin1 overexpressing cells exhibited a moderate activation of FAK (Y397), AKT (Ser473) and Src, (non-adherent conditions), although the response was weaker than under fibronectin conditions (Fig. 5C). Analysis of the anchorage independent phosphorylation of these proteins revealed a significant time-dependent increase in phosphorylation of FAK, AKT and Src in talin1-overexpressing cells, that was paralleled by a reduction in caspase-3 activation (Fig. 5C, right panel). Considering the evidence that ILK-1 is an effective signaling mediator of anoikis resistance (20), we also examined GSK3- β activation, a direct target for ILK-1, under non-adherent conditions. Talin1 overexpressing cells exhibited increased phosphorylation of GSK3 β and reduced caspase-3 cleavage compared to vector control cells, indicating anoikis suppression (Fig. 5C, right panel). Resistance to anoikis is recognized as a critical mechanism underlying tumor cell metastatic dissemination (4). Thus subsequent studies pursued the functional characterization of talin1 in determining the metastatic potential of prostate cancer cells *in vivo*. Talin1 loss in prostate cancer cells led to a significantly reduced number of metastatic tumor lesions (to the lungs) (Fig. 5D).

AKT Involvement in Talin1 Mediated Migration and Invasion but not Adhesion

To determine whether AKT activation is an integral part of talin1 intracellular signaling, the consequences of AKT inhibition on talin1-mediated biological effects were examined. As shown on Supplemental Figure 2, AKT inhibition had no significant effect on the adhesion potential of talin1 overexpressing prostate cancer cells, on either fibronectin or laminin-coated matrix. In the presence of the AKT inhibitor, both the migration potential and invasion ability of talin overexpressing cells (Fig. 2S) were significantly suppressed compared to the vector control cells ($p < 0.01$).

DISCUSSION

Tumor cells develop mechanisms to resist anoikis, which enables their survival after detachment from the primary site and travel through the lymphatic and circulatory systems to distant organs (4). The present study identifies talin1 as a novel regulator of prostate cancer cell invasion and metastatic potential via its survival signaling by activating the ECM-integrin mediated signaling and promoting anoikis resistance. Talin1 overexpression significantly enhanced the migration and invasion potential of human prostate cancer cells in an AKT dependent manner. In contrast, loss of talin1 led to a diminished invasion potential and *in vivo* metastatic ability of prostate cancer cells. These results are in accord with a previous screening reporting that highly metastatic cells expressed significantly high levels of talin1 (>16 fold, 2nd highest out of 440 proteins screened) compared to less metastatic cells (21). Interestingly enough, talin1 mRNA has been shown to be downregulated by androgens in primary prostate cancer cells(22). Our *in vivo* findings in the TRAMP model of prostate tumorigenesis reveal a positive correlation between talin1 immunoreactivity and prostate cancer progression to metastasis. A dramatic increase in talin-1 expression was detected in prostate tumors from 12wk TRAMP mice and talin1 levels were further increased with tumor progression to advanced metastatic disease. Taken together, these evidences support an indirect link between talin1 and prostate cancer metastasis and emergence to androgen-independence.

Overexpressing talin1 in prostate cancer cells led to activation of FAK/AKT signaling via both an ECM-dependent and -independent mechanism. Gaining support from evidence that AKT survival signaling is causally linked to anoikis resistance in detached cells (23,24), our data indicate that talin1 promotes tumor cells to metastasize by enhancing their local invasive properties and survival after detachment from the primary tumor site via activation of FAK and AKT signaling. This resonates with a similar role assigned to another key focal adhesion protein, paxillin, in different tumors. Indeed, overexpression of paxillin correlates with metastatic and invasion properties in hepatocellular carcinoma (25). Recruitment of FAK and paxillin to β 1 integrin promotes cancer cell migration through MAPK activation (26). The present findings suggest that talin1 might not be causally involved in primary tumor development and growth, but rather in promoting local invasion, as well as distant metastasis, via targeting the ECM-integrin mediated signaling and resistance to anoikis.

Resistance to anoikis, potentially conferred by talin1, is not a selective advantage during tumor growth in an ECM-rich microenvironment; rather during the invasion through vasculature during metastasis. Resistance to anoikis could predict a greater ability to form metastatic lesions. The idea resonates with the evidence gathered from the analysis of human prostate cancer specimens. The highest talin1 protein expression was found in metastatic lesions compared to benign areas and primary prostate tumor sites (Table 1a). Interestingly enough there was a gradient of increasing expression within the primary tumors of increasing Gleason score (Table1b). This points to a promising value of talin1 expression in primary tumors as a predictor of metastatic potential, since prostate tumors with high Gleason score (>8) are pathologically recognized as high risk adenocarcinoma and those patients have limitations in treatment options due to higher incidence of distant metastasis that significantly limits prognosis (27). A similar functional contribution in enhancing metastasis but not primary tumor growth, was demonstrated by the apoptotic suppressor of cytoskeleton-dependent death, Bcl-XI during mammary carcinogenesis (28).

Mechanistic dissection revealed that talin1 promotes ILK-1 binding to integrin β 3 subunit; this evidence implicates ILK-1 as an intracellular effector of talin1 signaling, activated upstream of the AKT survival pathway. Integrin-linked kinase (ILK) is a serine/threonine protein kinase that interacts with cytoplasmic domain of β 1-integrin and β 3-integrin and has been functionally linked to integrin and Wnt signaling pathways (29-31). ILK regulates several integrin-mediated

cellular processes including cell adhesion, fibronectin-ECM assembly and anchorage-dependent cell growth (30,32,33). Upon cell adhesion, ILK is transiently activated and directly phosphorylates AKT Ser473 (34) and glycogen synthase kinase-3 (GSK3) (32). In contrast, inhibiting ILK in cancer cells inhibits AKT phosphorylation and cell survival. ILK-1 mediates anoikis resistance even without activation of integrin/ECM signals, possibly via recruiting through α -parvin-mediated targeting of AKT to lipid rafts (20,35,36). Our *in vitro* data suggest that talin1 facilitates direct ECM-epithelial interaction and confers anoikis resistance.

Based on these findings we propose that talin1 is responsible for the acquisition of the primary prostate tumor cell invasive and metastatic properties leading to metastasis. In the schematic scenario shown on Supplemental Figure 3 (Suppl. Data), under adherent conditions, talin1 facilitates integrin signaling and its link to the ECM. Talin1 binding to β integrin recruits the focal adhesion proteins ILK, FAK and Src, towards activation of the downstream signals such as AKT and ERK. These signaling events promote cell survival, invasion and angiogenesis. Under non-adherent conditions, talin1 stimulates FAK, Src and GSK3 β -independent of integrin signaling and confers resistance to anoikis, leading to metastatic spread (Supplemental Figure 3). Our attempts to analyze the direct interaction of talin1 with ILK-1 or β integrin did not provide clear evidence of such interactions under non-adherent conditions. This might be attributed to weak “bonding” interactions relative to the adherent focal adhesion complex by additional proteins responsible for transducing talin1 signaling under non-adherent conditions.

The clinical relevance of our findings relates to the significant increase in talin1 expression in primary tumors and metastatic prostate cancer, compared to benign and normal prostate. The metastatic specimens exhibited significantly higher talin1 levels compared to primary prostate tumors, implicating an involvement of talin1 in the metastatic process. These results suggest that talin1 may have diagnostic value in prostate cancer detection and clinical outcome. Ongoing studies focus on a correlation between talin1 expression with serum PSA levels, Gleason grade and patient (disease-free) survival in a large cohort of prostate cancer patients, which may define the value of talin1 as a cancer metastasis marker. The interaction with other talin1 binding candidates including paxillin, and vinculin, and the impact of such interactions on the phosphorylation status of critical downstream anoikis-repression signaling effectors is the focus of ongoing studies. Since talin1 contains multiple phosphorylation sites including PKA, PKC and GSK3, as predicted by mass spectrometry (37), it is tempting to propose a potential strategy to target these phosphorylation sites to block talin1-mediated survival signaling in tumor cells. Further dissection of the functional contribution of talin1 in dictating tumor cell and endothelial survival outcomes, may provide new opportunities for therapeutic targeting of metastatic prostate cancer.

In summary, the evidence presented supports a regulatory role for talin1 in tumor cell invasion and prostate cancer metastasis via conferring anoikis resistance. Future studies will pursue the generation of a conditional knockout mouse model of talin1, selectively targeting talin1 gene expression in prostate epithelial cells and its crossing with a transgenic mouse model of prostate cancer.

Supplementary Material

Refer to Web version on PubMed Central for supplementary material.

Acknowledgments

This work was supported by an NIH R01 CA107575-06 grant (NK), a Markey Cancer Foundation Grant (NK) and an American Cancer Society IRG Grant (ROM). Shinichi Sakamoto is an American Urological Association Foundation Research Scholar. The authors acknowledge the assistance of Dr. Hong Pu with the animal experiments; Matthew Martelli for the initial contribution to the *in vitro* analysis of talin1; Dr. Barbara Foster (Roswell Park Cancer Institute),

for expert help with the TRAMP mouse model and specimen acquisition; Dr. Steven Schwarze (Department of Biochemistry) and Dr. Chendil Damodaran (College of Health Science) for useful discussions and Lorie Howard for assistance with the manuscript submission process.

Abbreviations

ECM	extracellular matrix
FAK	focal adhesion kinase
TRAMP	transgenic adenocarcinoma of the mouse prostate
BSA	bovine serum albumin
SDS-PAGE	sodium dodecyl sulfate polyacrylamide gel electrophoresis
pEGFP	red-shifted variant of wild-type Green fluorescence protein
DAPI	4',6-diamidino-2-phenylindole
poly-HEMA	poly (2-hydroxyethyl) methacrylate
TBST	TRIS buffered saline with Tween 20
BPH	Benign Prostate Hyperplasia

REFERENCES

1. Fornaro M, Manes T, Languino LR. Integrins and prostate cancer metastases. *Cancer Metastasis Rev* 2001;20(34):321–31. [PubMed: 12085969]
2. McKenzie S, Kyprianou N. Apoptosis evasion: the role of survival pathways in prostate cancer progression and therapeutic resistance. *J Cell Biochem* 2006;97(1):18–32. [PubMed: 16216007]
3. Frisch SM, Screaton RA. Anoikis mechanisms. *Current opinion in cell biology* 2001;13(5):555–62. [PubMed: 11544023]
4. Rennebeck G, Martelli M, Kyprianou N. Anoikis and survival connections in the tumor microenvironment: is there a role in prostate cancer metastasis? *Cancer research* 2005;65(24):11230–5. [PubMed: 16357123]
5. Giancotti FG, Ruoslahti E. Integrin signaling. *Science* 1999;285(5430):1028–32. [PubMed: 10446041]
6. Calderwood DA. Integrin activation. *Journal of cell science* 2004;117(Pt 5):657–66. [PubMed: 14754902]
7. Alam N, Goel HL, Zarif MJ, Butterfield JE, Perkins HM, Sansoucy BG, Sawyer TK, Languino LR. The integrin-growth factor receptor duet. *J. Cell Physiology* 2007;213(3):649–53.
8. Fornaro MMT, Languino LR. Integrins and prostate cancer metastases. *Cancer Metastasis Rev* 2001;20(34):321–31. [PubMed: 12085969]
9. Tanentzapf G, Brown NH. An interaction between integrin and the talin FERM domain mediates integrin activation but not linkage to the cytoskeleton. *Nature cell biology* 2006;8(6):601–6.
10. Brown NHGS, Rickoll WL, Fessler LI, Prout M, White RA, Fristrom JW. Talin is essential for integrin function in *Drosophila*. *Dev Cell* 2002;3(4):569–79. [PubMed: 12408808]
11. Becam IE, Tanentzapf G, Lepesant JA, Brown NH, Huynh JR. Integrin-independent repression of cadherin transcription by talin during axis formation in *Drosophila*. *Nature cell biology* 2005;7(5):510–6.
12. Keledjian K, Garrison JB, Kyprianou N. Doxazosin inhibits human vascular endothelial cell adhesion, migration, and invasion. *Journal of cellular biochemistry* 2005;94(2):374–88. [PubMed: 15526277]
13. Hu Y, Qiao L, Wang S, et al. 3-(Hydroxymethyl)-bearing phosphatidylinositol ether lipid analogues and carbonate surrogates block PI3-K, Akt, and cancer cell growth. *Journal of medicinal chemistry* 2000;43(16):3045–51. [PubMed: 10956212]
14. Gingrich JRBR, Foster BA, Greenberg NM. Pathologic progression of autochthonous prostate cancer in the TRAMP model. *Prostate Cancer Prostatic Dis* 1999;2(2):70–5. [PubMed: 12496841]

15. Greenberg NMDF, Finegold MJ, Medina D, Tilley WD, Aspinall JO, Cunha GR, Donjacour AA, Matusik RJ, Rosen JM. Prostate cancer in a transgenic mouse. *Proc Natl Acad Sci U S A* 1995;92(8):3439–43. [PubMed: 7724580]
16. Zeng L, Rowland RG, Lele SM, Kyprianou N. Apoptosis incidence and protein expression of p53, TGF-beta receptor II, p27Kip1, and Smad4 in benign, premalignant, and malignant human prostate. *Human pathology* 2004;35(3):290–7. [PubMed: 15017584]
17. Camp RL, Chung GG, Rimm DL. Automated subcellular localization and quantification of protein expression in tissue microarrays. *Nature medicine* 2002;8(11):1323–7.
18. Bouchard VDM, Thibodeau S, Laquerre V, Fujita N, Tsuruo T, Beaulieu JF, Gauthier R, Vézina A, Villeneuve L, Vachon PH. Fak/Src signaling in human intestinal epithelial cell survival and anoikis: differentiation state-specific uncoupling with the PI3-K/Akt-1 and MEK/Erk pathways. *J Cell Physiol* 2007;212(3):717–28. [PubMed: 17443665]
19. Calderwood DA, Yan B, de Pereda JM, et al. The phosphotyrosine binding-like domain of talin activates integrins. *The Journal of biological chemistry* 2002;277(24):21749–58. [PubMed: 11932255]
20. Hannigan G, Troussard AA, Dedhar S. Integrin-linked kinase: a cancer therapeutic target unique among its ILK. *Nature reviews* 2005;5(1):51–63.
21. Everley PAKJ, Zetter BR, Gygi SP. Quantitative cancer proteomics: stable isotope labeling with amino acids in cell culture (SILAC) as a tool for prostate cancer research. *Mol Cell Proteomics* 2004;3(7):729–35. [PubMed: 15102926]
22. Betts AMCG, Neal DE, Robson CN. Paracrine regulation of talin mRNA expression by androgen in human prostate. *FEBS Lett* 1998;434(12):66–70. [PubMed: 9738453]
23. Chang LCHC, Cheng CH, Chen BH, Chen HC. Differential effect of the focal adhesion kinase Y397F mutant on v-Src-stimulated cell invasion and tumor growth. *J Biomed Sci* 2005;12(4):571–85. [PubMed: 16132110]
24. Irie HY, Pearlman RV, Grueneberg D, et al. Distinct roles of Akt1 and Akt2 in regulating cell migration and epithelial-mesenchymal transition. *J Cell Biol* 2005;171(6):1023–34. [PubMed: 16365168]
25. Li HGXD, Shen XM, Li HH, Zeng H, Zeng YJ. Clinicopathological significance of expression of paxillin, syndecan-1 and EMMPRIN in hepatocellular carcinoma. *World J Gastroenterol* 2005;11(10):1445–51. [PubMed: 15770719]
26. Crowe DLOA. Recruitment of focal adhesion kinase and paxillin to beta1 integrin promotes cancer cell migration via mitogen activated protein kinase activation. *BMC Cancer* 2004;4:18. [PubMed: 15132756]
27. Partin AW, Kattan MW, Subong EN, et al. Combination of prostate specific antigen, clinical stage and Gleason score to predict pathological stage of localized prostate cancer. A multi-institutional update. *JAMA* 1997;277(18):1445–51. [PubMed: 9145716]
28. Martin SS, Ridgeway AG, Pinkas J, et al. A cytoskeleton-based functional genetic screen identifies Bcl-xL as an enhancer of metastasis, but not primary tumor growth. *Oncogene* 2004;23(26):4641–5. [PubMed: 15064711]
29. Wu C, Dedhar S. Integrin-linked kinase (ILK) and its interactors: a new paradigm for the coupling of extracellular matrix to actin cytoskeleton and signaling complexes. *The Journal of cell biology* 2001;155(4):505–10. [PubMed: 11696562]
30. Hannigan GE, Leung-Hagesteijn C, Fitz-Gibbon L, et al. Regulation of cell adhesion and anchorage-dependent growth by a new beta 1-integrin-linked protein kinase. *Nature* 1996;379(6560):91–6. [PubMed: 8538749]
31. Li F, Liu J, Mayne R, Wu C. Identification and characterization of a mouse protein kinase that is highly homologous to human integrin-linked kinase. *Biochimica et biophysica acta* 1997;1358(3):215–20. [PubMed: 9366252]
32. Cieslik K, Zembowicz A, Tang JL, Wu KK. Transcriptional regulation of endothelial nitric-oxide synthase by lysophosphatidylcholine. *The Journal of biological chemistry* 1998;273(24):14885–90. [PubMed: 9614091]
33. Radeva G, Petrocelli T, Behrend E, et al. Overexpression of the integrin-linked kinase promotes anchorage-independent cell cycle progression. *The Journal of biological chemistry* 1997;272(21):13937–44. [PubMed: 9153256]

34. Lynch DK, Ellis CA, Edwards PA, Hiles ID. Integrin-linked kinase regulates phosphorylation of serine 473 of protein kinase B by an indirect mechanism. *Oncogene* 1999;18(56):8024–32. [PubMed: 10637513]
35. Attwell S, Roskelley C, Dedhar S. The integrin-linked kinase (ILK) suppresses anoikis. *Oncogene* 2000;19(33):3811–5. [PubMed: 10949937]
36. Fukuda T, Chen K, Shi X, Wu C. PINCH-1 is an obligate partner of integrin-linked kinase (ILK) functioning in cell shape modulation, motility, and survival. *The Journal of biological chemistry* 2003;278(51):51324–33. [PubMed: 14551191]
37. Ratnikov B, Ptak C, Han J, Shabanowitz J, Hunt DF, Ginsberg MH. Talin phosphorylation sites mapped by mass spectrometry. *Journal of cell science* 2005;118(Pt 21):4921–3. [PubMed: 16254238]

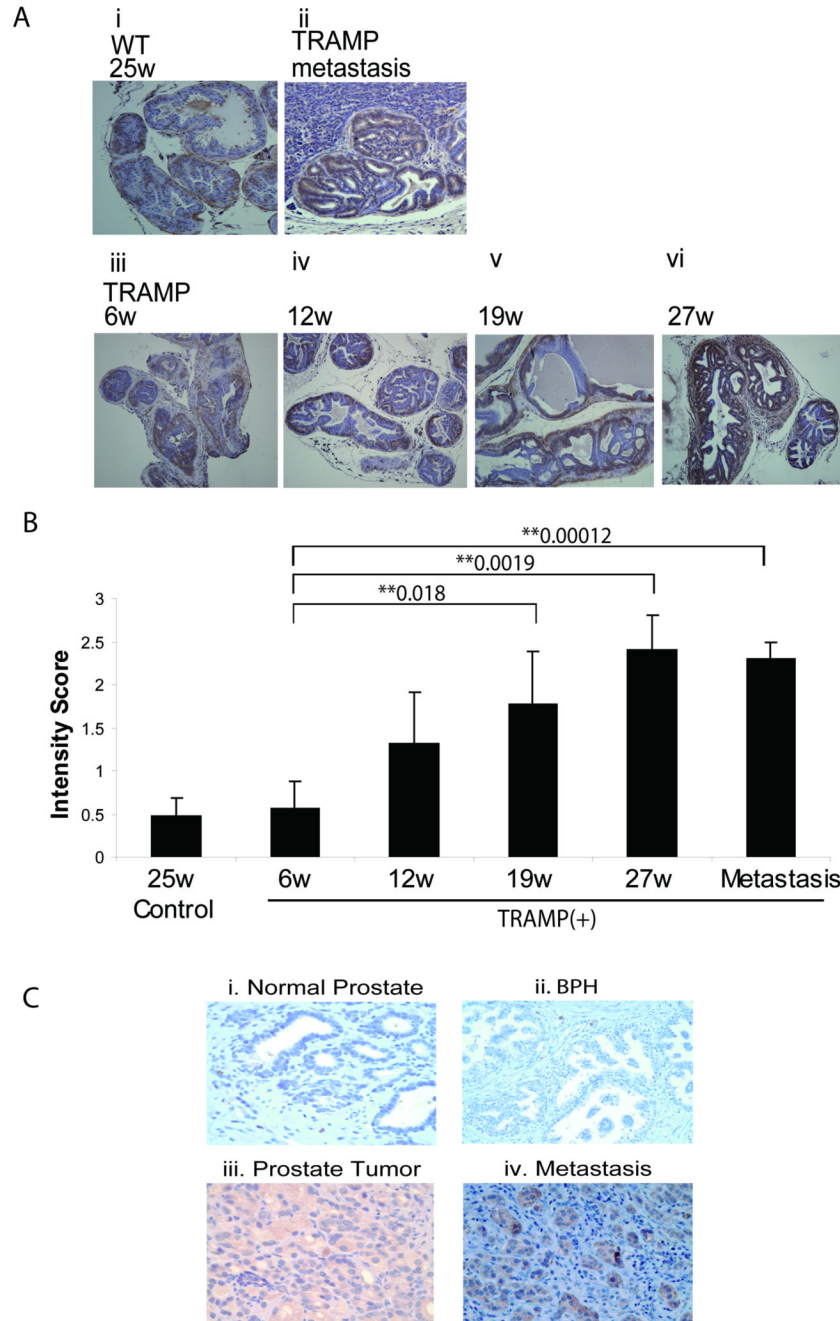


Figure 1. Talin1 Profiling during Prostate Tumor Progression in the TRAMP Model and human Prostate Cancer Specimens

Panel (A), Talin1 expression was analyzed in paraffin-embedded prostate tissue specimens from TRAMP mice and control age-matched mice (6-27 wks). A strong immunoreactivity for talin1 was detected in prostate tumors derived from both 19wk and 27wk TRAMP mice, subpanels (iv) and (v), respectively. Sub-panel (ii) represents a metastatic lesion to the liver in a TRAMP mouse (27wks). **Panel (B)**, The intensity of IHC staining (H) was calculated by $P = \text{Percentage of staining} \times I \text{ intensity (1-3)}$. The numerical data reveal a positive correlation between increasing tumor grade and progression to metastasis and increased talin expression. (*) and (**) indicate statistical difference at $p \text{ value} < 0.05$ and < 0.01 , respectively, compared

to specimens from control mice. **Panel (C)**; Talin1 immunoreactivity was analyzed in paraffin-embedded prostate tissue specimens from normal (i), BPH (ii), primary prostate tumors (iii) and metastasis (iv).

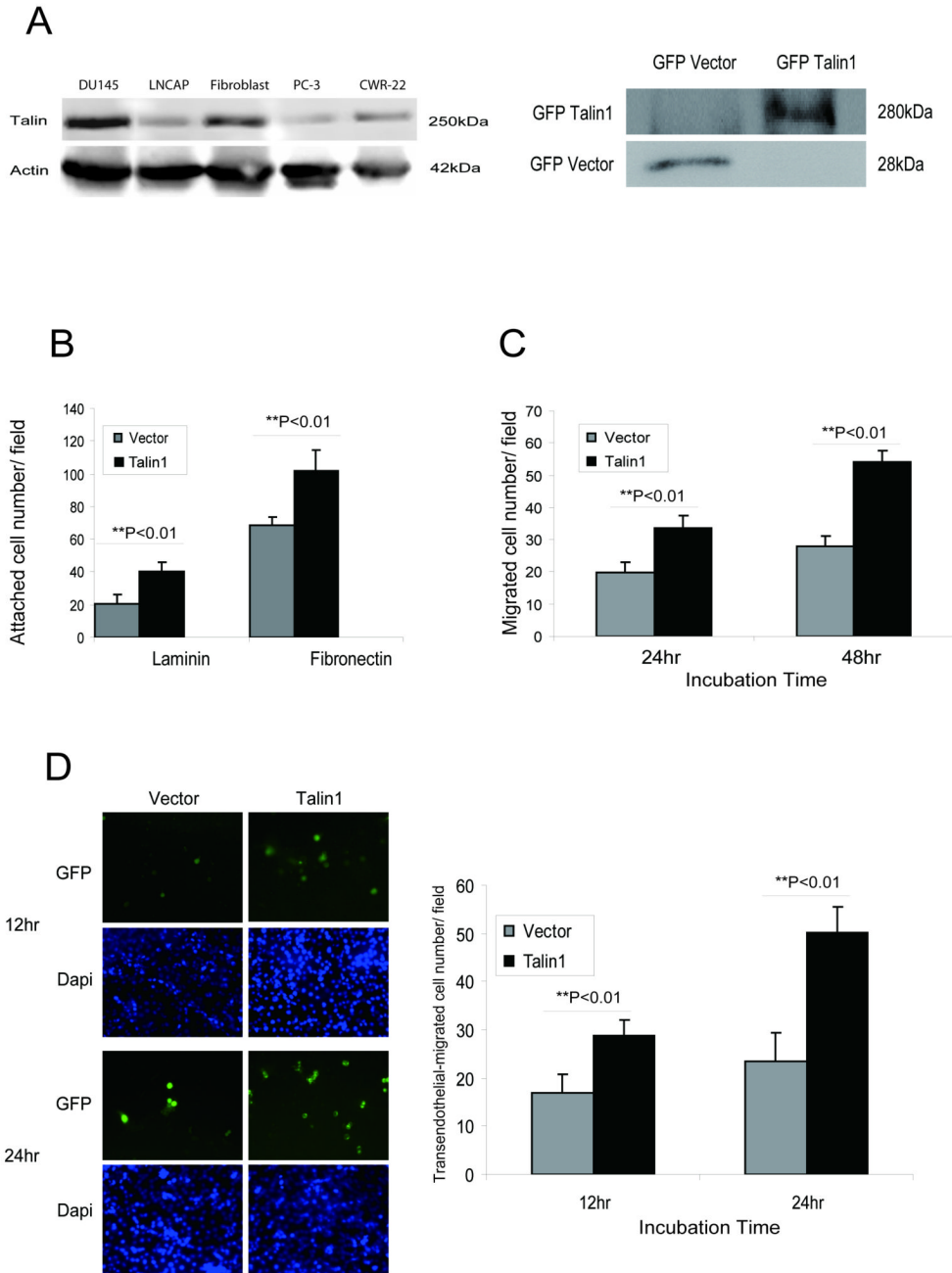


Figure 2. Talin1 Enhances Cell Adhesion, Migration and Invasion

Panel A, Talin1 endogenous expression in human prostate cancer cell lines; actin expression is used as a loading control. Bands detected indicate GFP-talin1 (280kDa) and GFP-vector protein (28kDa) respectively. **Panel B**, Cell adhesion potential was comparatively analyzed in laminin or fibronectin-coated plates in PC-3 GFP vector control and PC-3 GFP- talin1 cloned transfectants. Values represent the mean from three independent experiments performed duplicate \pm SEM. **Panel C**, PC-3 cells were subjected to wounding and migrating cells were counted under the microscope in three independent fields (3 wells/condition). **Panel D**, The transendothelial migration assay was performed using HBMECs, and either PC-3 GFP-vector or PC-3 GFP-talin1 expressing cells, as described in “Materials and Methods”. Green and blue

staining indicated GFP vector/talin1 cells and DAPI nuclear staining, respectively. Numerical data represent values from three independent experiments \pm SEM.

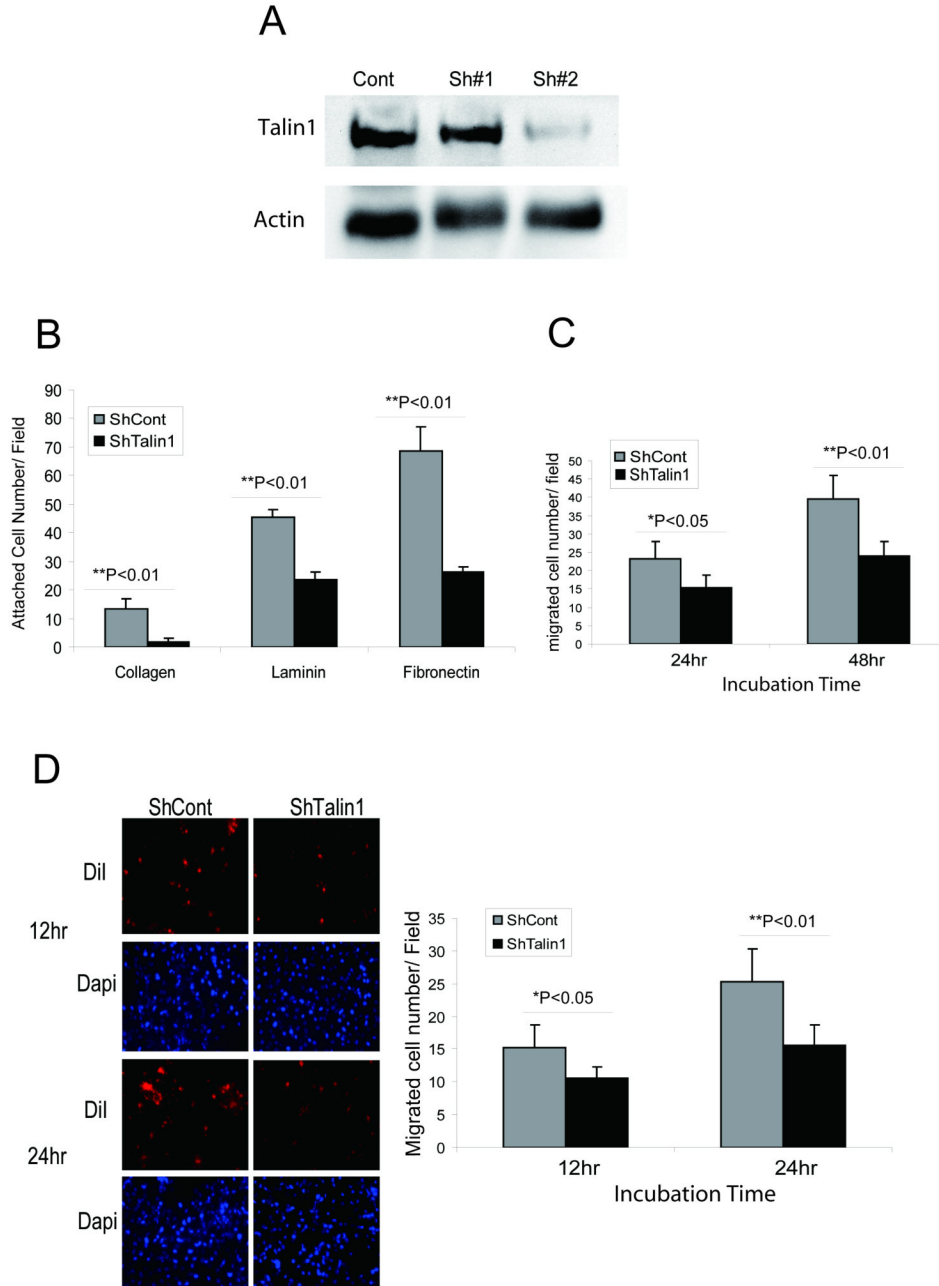


Figure 3. Talin1 Loss Decreases Cell Adhesion, Migration and Invasion

Panel A, ShRNA talin1 stable cell line was established in DU-145 cells. **Panel B**, ShRNA vector and ShRNA-talin1 transfectant cells were comparatively analyzed for their adhesion potential (as described above). Values represent mean \pm SEM from three independent experiments. **Panel C**, Talin1 silencing reduces DU-145 cell migration ability. Cells were subjected to wounding and their migration potential was evaluated; the number of migrating cells was counted under the microscope in three independent fields ($40\times$ ***) per well (3 wells/condition). **Panel D**, Loss of talin1 inhibits prostate tumor cell invasion. Transendothelial migration assay was conducted using HBMEC (human brain microvascular endothelial cell) DU-145 vector and ShRNA Talin1 stable cell line. The number of invading cells (red) was

determined under confocal microscopy after 12 and 24 hrs. Blue color represents DAPI nuclear staining.

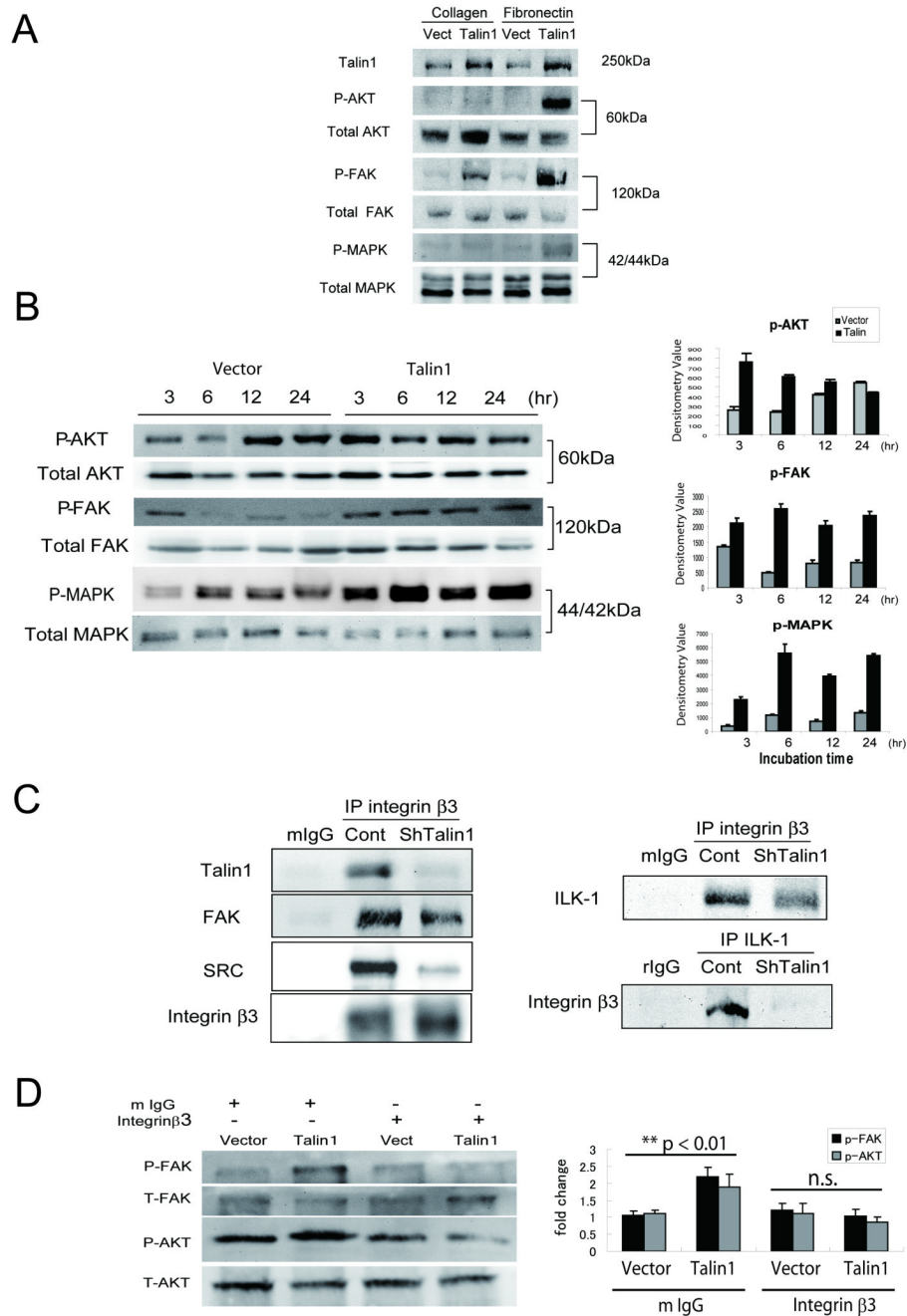


Figure 4. Talin1 Mediates ECM-dependent Activation of FAK/AKT Pathway

Panel A, After adherence of GFP-talin1 and vector-transfected PC-3 cells on either collagen or fibronectin plates (6hrs), cells were lysed and subjected to Western blot analysis. Levels of total and phosphorylated AKT (Ser473), FAK (Y397) and MAPK proteins were detected using respective antibodies. **Panel B**, Phosphorylation of AKT (Ser473), FAK(Y397) and MAPK were evaluated after (6hr) adherence to fibronectin. Quantification of phosphorylation was performed by densitometry (as shown on the right). **Panel C**, ShTalin1 DU-145 cells were subjected to immunoprecipitation using the integrin $\beta 3$ antibody or the ILK-1 antibody. As controls, proteins were precipitated with the control IgG derived from the same species plus the secondary antibody (protein G/A). Talin1, total FAK and SRC binding were detected by

Western blotting. Binding of ILK-1 or integrin β 3 was determined using the respective antibodies (right panel). **Panel D**, GFP vector and talin1 expressing PC-3 cells were plated on fibronectin-coated plate incubated with mouse IgG or integrin β 3 (blocking) antibodies (20 μ g/ml); The total proteins and phosphorylated forms of FAK and AKT were determined by immunoblotting after 6hrs of plating.

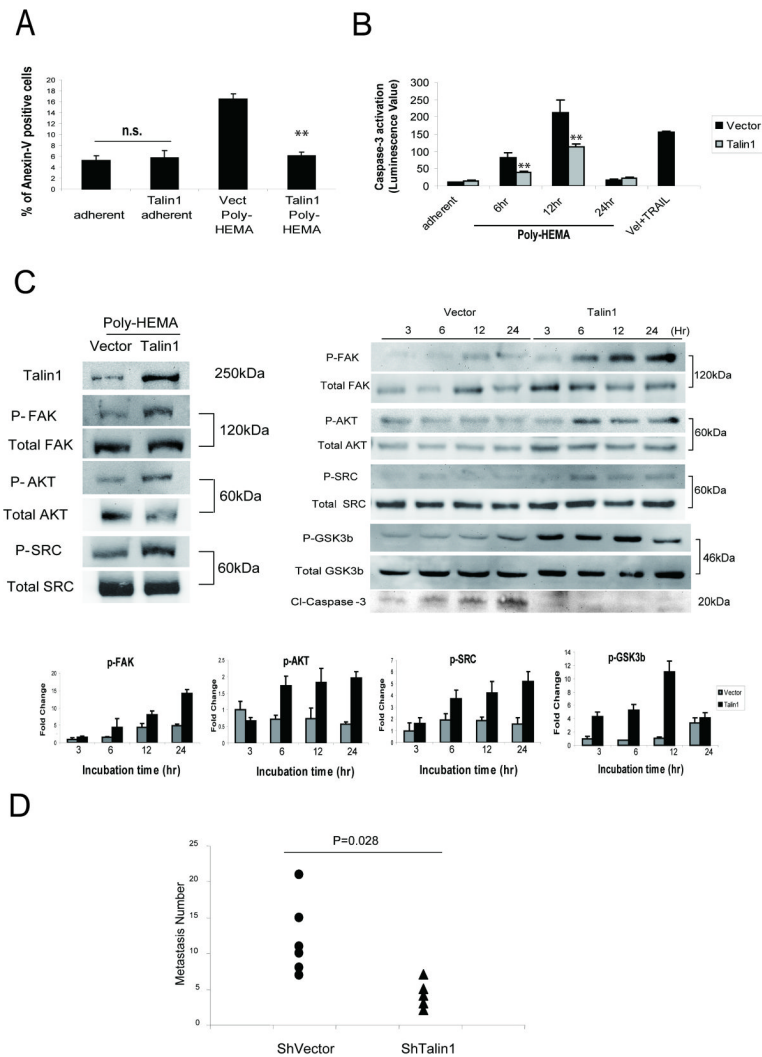


Figure 5. Talin1 Mediates Anoikis Resistance

Panel A, GFP-talin1 and vector PC-3 cells were kept in suspension conditions using Poly-HEMA coated plates for 24hr and subjected to Flow Cytometry using AnnexinV antibody. **Panel B**, Caspase-3 activation was measured in Poly-HEMA suspension conditions after 6, 12 and 24hrs as described in “Materials and Methods”. GFP talin1 and GFP vector cells were also treated with TRAIL (100ng/ml) plus Velcade (100nM) (positive control). Values indicate the mean from two independent experiments performed in triplicate \pm SEM. (***) indicates statistically significant difference at $p < 0.01$ **Panel C**, GFP-talin1 and vector PC-3 cells were kept in suspension conditions and after 24hrs, cells were lysed and subjected to Western blotting. Expression of total protein and phosphorylated forms of AKT (Ser473), FAK (Y397) and p42/44MAPK were detected using respective antibodies (left panel). Levels of total and phosphorylated AKT (Ser473), FAK (Y397), SRC and GSK3 β as well as cleaved caspase-3, were assessed during different time points (3-24hr) (right panel). The phosphorylation status of individual proteins was evaluated by densitometry (lower panel). **Panel D**, Experimental metastasis assay. Nude mice were injected intravenously in the tail vein with prostate cancer cells, DU-145 ShVector, (n=6) and DU-145 shRNA talin1, [n=5, (2×10^6 /mouse)]. At 5-wks post-inoculation, lungs were dissected and metastatic lesions were counted. Talin 1 loss led to a significantly reduced number of metastatic lesions to the lungs (P =0.028).

Table 1
Expression of Talin1 in Human Prostate Cancer

(a) Talin1 protein expression was evaluated by computer-based imaging. Specimens included normal prostate, normal tissue adjacent to tumor foci, benign prostate hyperplasia, BPH; primary prostate tumor and lymph node metastasis. (*) and (**) indicate statistical difference at p value<0.05 and <0.01, respectively, compared to normal prostate. Table 1a Quantitative analysis of talin 1 expression in human prostate tissue (b) Comparative evaluation of talin1 levels in human primary prostate cancer specimens (Gleason 6/7) and poorly differentiated tumors (Gleason Score >8; 8, 9, 8/9). (*) and (**) indicate statistical differences at p-value<0.05 and p<0.01, respectively, compared to moderately differentiated tumors (Gleason Score 6/7). Table 1b Talin 1 expression in primary prostate tumor

Specime	(n)	Intensity	P-value
Normal	(42)	155.4±5.3	
Adjacent	(101)	150.2±8.3	*0.017
BPH	(56)	155.2±6.3	0.319
Primary Tumor	(34)	162.2±7.8	**0.00028
Metastasis	(74)	167.3±7.9	**0.0000009

**0.0030

Tumor Grade	(n)	Intensity	P-value
Gleason 6/7	(15)	154.2±8.7	
Gleson 8	(9)	163.0±10.3	*0.0327
Gleson 9	(10)	167.1±4.5	*0.0005
Gleson 8/9	(19)	164.9±8.2	**0.0009